Passage of soft pathogens through microfiltration membranes scales with transmembrane pressure

www.elsevier.com/locate/memsci

Passage of soft pathogens through microfiltration membranes scales with transmembrane pressure

Alexander Helling, Alexander Kubicka, Iwan A.T. Schaap, Milan Polakovic, Björn Hansmann, Holger Thiess, Jochen Strube, Volkmar Thom

PII: S0376-7388(16)30887-0
DOI: http://dx.doi.org/10.1016/j.memsci.2016.08.016
Reference: MEMSCI14666

To appear in: *Journal of Membrane Science*

Received date: 4 July 2016
Revised date: 12 August 2016
Accepted date: 13 August 2016

Cite this article as: Alexander Helling, Alexander Kubicka, Iwan A.T. Schaap, Milan Polakovic, Björn Hansmann, Holger Thiess, Jochen Strube and Volkmar Thom, Passage of soft pathogens through microfiltration membranes scales with transmembrane pressure, *Journal of Membrane Science* http://dx.doi.org/10.1016/j.memsci.2016.08.016

Passage of soft pathogens through microfiltration membranes scales with transmembrane pressure

Alexander Helling[1,2], Alexander Kubicka[3], Iwan A. T. Schaap[4], Milan Polakovic[2], Björn Hansmann[1], Holger Thiess[3], Jochen Strube[3], Volkmar Thom[1*]

[1]Sartorius Stedim Biotech GmbH, August-Spindler-Straße 11, 37079 Goettingen, Germany
[2]Department of Chemical and Biochemical Engineering, Institute of Chemical and Environmental Engineering, Faculty of Chemical and Food Technology, Slovak University of Technology, 81237 Bratislava, Slovakia
[3]Institute for Separation and Process Technology, Faculty of Mathematics/Computer Science and Mechanical Engineering, Clausthal University of Technology, 38678 Clausthal-Zellerfeld, Germany
[4]Institute of Biological Chemistry, Biophysics and Bioengineering, School of Engineering and Physical Sciences, Heriot-Watt University, Edinburgh EH14 4AS, UK

[*]**Corresponding author.** V. Thom. Sartorius Stedim Biotech GmbH. August-Spindler-Straße 11. 37079 Göttingen, Germany. volkmar.thom@sartorius-stedim.com

Abstract

This experimental study elucidates the impact of transmembrane pressure and particle deformability on the retention of biological and non-biological particles by porous microfiltration polymer membranes in dead-end filtration processes. Bacteriophages, mycoplasma, common bacteria and polystyrene model particles, ranging from 0.02 µm to 1.5 µm in particle diameter, were chosen due to their industrial relevance as well as due to their expected differences in deformability. For each particle type, precipitation cast polyethersulfone membranes with a sponge-like structure were tailor-made in order to achieve two levels of retention for the respective particle type. The transmembrane pressure was varied from 10 to 950 kPa and the stiffness of the particles was measured with atomic force microscopy. A good correlation between particle stiffness on the one hand and the impact of transmembrane pressure on particle retention on the other hand was observed. The present study suggests that mycoplasma and Gram-negative bacteria are easily deformable at low forces, which explains that they are thus able to squeeze through membrane pores when transmembrane pressure is increased. In contrast, for the relatively stiff Gram-positive bacteria, much higher transmembrane pressures were needed to show a retention decrease. Bacteriophages and polystyrene beads did not show higher passage at the exerted transmembrane pressures.

Keywords: Bacteria, microfiltration, virusfiltration, retention, phages, transmembrane pressure, deformability, softness, AFM, deformation, Mycoplasma, Young's modulus

Abbreviations

AFM - Atomic force microscopy
ASTM - American Society for Testing and Materials

ATCC - American Type Culture Collection

DLS - Dynamic light scattering

LRV - Log reduction value

PES - Polyethersulfone

PSD - Particle size distribution

TMP - Transmembrane pressure

TSB - Trypticase soy broth

1 Introduction

The manufacture of biopharmaceutical products such as antibodies, vaccines or active pharmaceutical ingredients underlies strict requirements to guarantee patient safety. A prerequisite for a safe product is a contaminant-free sterile preparation in both upstream and downstream processing. Media ingredients, buffers, cell lines and the operators themselves are potential sources for biological contaminations like bacteriophages, viruses, mycoplasma and common bacteria [1–4]. Product contamination will lead to loss of product, and in severe cases to a shutdown of the whole facility with impact on drug supply and thus patient safety [4–6]. Membrane filtration is established as the most economic and gentle method for size-based clearance of biological particle contaminations in biopharmaceutical processes streams [7]. Sieving is seen as the pre-dominant mechanism for particle clearance by filter membranes, which is true for viruses and bacteria equally [8–10]. A higher transmembrane pressure (TMP) can increase the flow rate and throughput of a filtration process.

However, the TMP can significantly impact the retentive performance of filter membranes used in biopharmaceutical applications [11,12]. Lebleu et al. [12] observed a decline in retention for E. coli filtered through 0.4 µm track-etched membranes from 20 to 100 kPa, reaching a plateau between 50 and 100 kPa. All Gram-negative species passed the membrane to a certain degree, while the Gram-positive ones were fully retained. Thus Lebleu et al. assumed Gram-negative bacteria to be flexible and Gram-positive to exhibit a lower flexibility. However, the membrane pore sizes might have been too small to see effects with the Gram-positive species. Folmsbee and Moussourakis [11] observed mycoplasma species to penetrate 0.1 µm rated microfiltration (MF) membranes at a TMP above 300 kPa. Sun et al. [13] presented a microfluidic platform, demonstrating the deformation of Gram-negative and Gram-positive bacteria. They observed that E. coli and B. subtilis, both approximately 1 µm in diameter, can travel into a tapered microfluidic channel that exhibits a characteristic orifice that is smaller than the particle diameter. The channel entrance had 1.4 µm, while the exit was 0.25 µm wide, which is in the range of common sterile filtration membrane pore size. The differential pressure between the entrance and exit was varied between 11 and 134 kPa. The higher the differential pressure the deeper the bacteria travelled into the channel while being deformed by the constraining channel walls. While Gram-negative E. coli travelled deeper into the tapered channel than Gram-positive B. subtilis, both bacteria were retained in a deformed state. This suggests that also Gram-positive bacteria species with a highly cross-linked and allegedly stiff cell wall are deformable.

Published data also indicate changes in virus and bacteriophage retention due to changes in TMP. Madaeni et al. [14] observed a decrease in poliovirus retention by 4% for a 0.22 µm rated, hydrophobic MF membrane when the TMP was increased from 25 to 200 kPa. They attributed this decrease to elevated concentration polarization at higher pressures and consequently higher particle concentrations in the permeate. Azari et al. [15] observed increased retention of φX174 by a 500 kDa UF membrane when the TMP was increased from 52 to 103 kPa. The authors explained this phenomenon by the presence of red blood cell haemolysate in the feed stream, which altered the accessibility of the membrane pores at higher pressure. Arkhangelsky et al. [16] observed a decrease of MS2 and φX174 phage retention up to 1 log unit using a 20 kDa UF membrane at transmembrane pressures higher than 100 kPa. A cause of this decrease could be an enlargement of the membrane pores rather than phage deformation.

The deformability of a particle depends on its structure and the material it is made of. Due to their small sizes, measuring stiffness of viruses and bacteria is challenging. Atomic force microscopy (AFM) has been used with increasing success to quantify the stiffness of single viruses, bacteria and eukaryotic cells [17–19]. The mechanical response is measured by indenting the objects with a probe that is mounted at the end of a flexible cantilever (typically 50-200 µm long). The obtained force versus indentation curve shows the relation between the exerted force and the deformation of the particle, from which its stiffness can be directly obtained. If the relation is linear, the stiffness (in N/m) can be directly extracted via Hooke's law. In most cases however, a model is applied to include non-linear contact conditions between the object and AFM probe and the shape and structure of the object itself [20]. Such approaches yield an intrinsic value for the elastic constant (Young's modulus) for the material the object is made of.

In this study the importance of the stiffness of pathogenic objects for their retention by membranes at different levels of TMP is addressed. Different to earlier approaches is that a unified technique was applied to measure the stiffness of a wide range of objects in the size range of 20 to 1500 nm, thus avoiding eventual variations caused by different measurement techniques. The retention of these particles by size exclusion membranes was measured for different TMP values, ranging from 10 to 950 kPa. Tailor-made model membranes with an overall low retention for the particles compared to respective commercial membranes are used, to be able to observe differences in retentive performance.

2 Experimental

2.1 Particles

The particles were chosen to span a wide range of particle types with various morphological characteristics (Table 1). Especially relevant for a biopharmaceutical process are mollicutes, referred to as mycoplasma, and common bacteria. One representative was chosen for each, mycoplasma, Gram-negative and Gram-positive bacteria, namely Acholeplasma laidlawii (ATCC 23206), Brevundimonas diminuta (ATCC 19146) and Staphylococcus epidermidis (ATCC 12228). Both, A. laidlawii and S. epidemidis exhibit nearly spherical shapes, whereas B. diminuta have a short rod like shape.

Pseudomonas phage PP7 (ATCC 15692-B2) was chosen as a virus surrogate exhibiting icosahedral protein capsids [21] for testing the retention of phages under increased pressures. Fluorescently labeled polystyrene latex beads (Fluoresbrite YG Carboxylate Microspheres 0.20µm, Polysciences Inc., USA) were chosen as hard spherical model particles.

The particle retention was calculated as the log reduction value (LRV) according to:

$$\mathrm{LRV} = \log_{10}\left(\frac{C_f}{C_p}\right) \quad (1)$$

with particle concentration in the feed C_f and particle concentration in permeate C_p.

Table 1: Characteristics of the biological and non-biological particles used.

Particle	Type	Gram stain	Shape
Acholeplasma laidlawii	Bacteria, Class: Mollicutes	Negative	Sphere
Brevundimonas diminuta	Bacteria, Class: Alphaproteobacteria	Negative	Short rod
Staphylococcus epidermidis	Bacteria, Class: Bacilli	Positive	Sphere
Pseudomonas phage PP7	ssRNA bacteriophage	-	Sphere, icosahedral
Polystyrene latex	Polymer beads	-	Sphere

2.2 Cultivations and counting of bacteria, phages and polystyrene beads

A. laidlawii

Under sterile conditions, a 5 mL aliquot of a mycoplasma stock culture A. laidlawii (ATCC 23206) (Mycoplasma Experience, UK), stored at -76 °C, was inoculated to 500 mL sterile, 0.1 µm filtered 30 g/L trypticase soy broth (TSB) (Merck KGaA, Germany) at pH 7.1±0.1. They were then cultivated for 24 hours under anaerobic conditions and 37°C without stirring.

The detection and quantification of A. laidlawii in a suspension was carried out using the membrane detection method. To determine the titer, 1 mL of a proper diluted bacteria suspension in a 0.1 M sodium phosphate buffer with pH 7.1±0.1 was filtered through an analytical detection membrane of 0.2 µm nominal pore size, which was then cultivated on Alert24 agar (Mycoplasma Experience, UK) for at least 3 days at 37 °C anaerobically. Produced colonies were then counted with the naked eye.

B. diminuta

B. diminuta (ATCC 19146) was cultivated in sterile, 0.1 µm filtered saline lactose broth (SLB), which consisted of 0.39 g/L DEV Lactose Broth (Merck KGaA, Germany) and 7.60 g/L NaCl (Merck KGaA, Germany) at pH 6.9±0.1. Under sterile conditions, 10 mL of SLB were inoculated with one cryogenic culture of B. diminuta at 30±2 °C for 24 hours. This pre-culture was transferred to 1 L sterile SLB and cultivated aerobically for further 24 hours at 30±2 °C in a magnetically stirred flask at 120 rpm.

To determine the titer of B. diminuta, 1 mL of a properly diluted bacteria suspension in a 0.1 M sodium phosphate buffer with pH 7.1±0.1 was filtered through an analytical detection membrane of 0.45 µm nominal pore size, which was then cultivated aerobically at 30 °C on trypticase soy agar (Sartorius Stedim Biotech, Germany) for at least 24 hours. Produced colonies were then counted with the naked eye.

S. epidermidis

Under sterile conditions, 10 mL TSB were inoculated with one cryogenic culture of S. epidermidis (ATCC 12228) at 37 °C for 24 h under aerobic conditions. This pre-culture was transferred to 500 mL sterile TSB and cultivated aerobically for further 24 h at 37 °C without stirring. The titer of S. epidermis was determined in the same way as for B. diminuta.

Pseudomonas phage PP7

Phages PP7 (ATCC 15692-B2) were produced in a Pseudomonas aeruginosa 1C (ATCC 15692) culture. P. aeruginosa was pre-cultivated in TSB for 24 hours at 37 °C and 150 rpm aerobically until a sufficient optical density was reached. A phage stock was added at a multiplicity of infection level between 0.5 and 4 and cultivated for another 24 hours at 37 °C and 150 rpm aerobically. The phage-bacteria-suspension was then centrifuged at 3076 g for 20 minutes to separate bacteria and PP7. The phage supernatant was filtered through a 0.2 µm membrane and the filtrate was used as a stock for further filtration retention experiments.

The detection and quantification of PP7 phage in a suspension was carried out with the plaque assay method. Dilutions of the phage suspension were mixed with a diluted P. aeruginosa pre-culture. The resulting suspensions were mixed with nutrient broth agar (Carl Roth, Germany) and poured onto the surface of a solid nutrient agar plate. The agar plates were incubated and grown to confluency over night at 37 °C and appearing plaques were counted.

Polystyrene beads

Fluorescently-dyed polystyrene beads (Fluoresbrite YG Carboxylate Microspheres 0.20 µm, Polysciences Inc., USA) with the mean particle size of 200 nm were quantified by fluorescence excitation at 468 nm and emission at 508 nm in 96 well plates with a Tecan M200 fluorescent microplate reader. The measurements and a calibration curve of beads was done in water containing 0.26 % sodium dodecyl sulfate (SDS). Detection of retention of up to 3 log units was possible using this technique.

2.3 Particle size determination by dynamic light scattering

The hydrodynamic diameters of the particles were determined by dynamic light scattering (DLS) using a Zetasizer Nano ZSP (Malvern Instruments, UK). The number distributions, mean diameters and standard deviations were considered.

Polystyrene beads were directly diluted 1000-fold in water containing 0.26 % SDS. Two samples of 2 mL were measured at 22 °C in triplicate with 14 sub-runs with the Zetasizer ZSP in disposable cuvettes.

Bacteria were cultivated in particle-free, 0.1 µm-filtered medium as described in chapter 2.2. After incubation, a sample of 10 mL was taken and filtered through a 5 µm cellulose acetate syringe filter (Sartorius Stedim Biotech GmbH, Germany) to eliminate larger aggregates. From this filtrate, two samples of 2 mL were measured without further purification at 22°C in triplicate with 14 sub-runs in disposable cuvettes. Since the refractive index of the bacteria used is unknown, it was set to 1.38 following the typical bacteria refractive index values of 1.36 – 1.41 [22–26]. Size calculations of A. laidlawii and S. epidermidis grown and measured in TSB were carried out using a dynamic viscosity of 1.031 cP, which was measured with an Ubbelohde viscometer at 22 °C. For size calculations of B. diminuta in SLB and polystyrene beads in water, the dynamic viscosity of water, 0.954 cP, was chosen.

The bacteriophage PP7 stock suspension was diluted in a 1:5 ratio with a 20 mM potassium phosphate buffer of pH 7.2. Three 0.1 µm filtered 1-mL samples were measured at 22 °C in triplicate with 14 sub-runs in disposable cuvettes. The protein refractive index value of 1.45 was chosen, since the phages are surrounded by a protein capsid.

2.4 Membrane pore size characterization by gas-liquid displacement porometry and bubble point testing

Pore sizes of the used membranes were determined with a Porolux 500 gas-liquid porometer (POROMETER nv, Belgium). Membranes of 25 mm diameter were wetted with “Porefil” perfluoroether wetting fluid with a surface tension of 16 mN/m (POROMETER nv, Belgium) and installed into the porometer measuring cell. Wetting liquid was displaced by nitrogen while pressure was increased. The pressure ramp was set to 1000 s/100 kPa. A gas-liquid displacement curve was captured and results were analyzed using the Porolux software.

The visual membrane bubble point was determined by immersing a water wetted membrane in a polycarbonate syringe filter housing (16517-E, Sartorius Stedim Biotech GmbH, Germany) into water. Air pressure was slowly increased with a manually operated pressure controller until a constant bubble column was visible and the respective pressure was recorded.

2.5 Atomic force microscopy measurements

Bacteria sample preparation

Microscopy coverslips with a diameter of 25 mm were plasma cleaned at 0.7 mbar for 60 seconds. Then, 400 µL of a 0.01% 150-300 kDa poly-L-lysine solution (Sigma-Aldrich, USA) were added on top of a coverslip to render the surface positively charged. After 15 minutes, the excess poly-L-lysine was removed and the coverslip was washed 3 times with 0.1 M sodium phosphate buffer of pH 7.1±0.1. Next, 400 µL of an undiluted bacteria suspension were added on top of the coverslip and left for 30 minutes. Live bacteria with a net negative charge were bound to the coverslip by static interactions with poly-L-lysine. To remove unbound bacteria, the coverslip was washed 3 times with the same

buffer. Then 400 µL of 0.005% DAPI (Applichem, USA) in water was added to the coverslip to label the DNA of the bacteria fluorescently for identification via fluorescence microscopy. For the experiment the coverslip was clamped into a coverslip holder and transferred to the AFM.

Phage sample preparation

PP7 phage stock suspension with a concentration of approximately 2×10^{11} plaque forming units per mL (PFU/mL) was diluted in the ratio of 1:100 with 10 mM Tris-HCl pH 8.1 containing 150 mM NaCl, 1 mM $MgCl_2$ and 10% glycerol. An aliquot of 0.5 µL of 5 mM $NiCl_2$ per 20 µL of this diluted phage suspension were added to facilitate phage adhesion. A freshly cleaved mica platelet was attached to a coverslip and clamped into a coverslip holder. Then 60 µL of the phage suspension were added on top of the mica platelet for 10 min. Unbound phages were removed by washing with buffer three times.

Polystyrene beads sample preparation

Carboxylated, fluorescently labeled polystyrene beads (Fluoresbrite YG Carboxylate Microspheres 0.20µm, Polysciences Inc., USA) were immobilized onto plasma cleaned glass coverslips. No further sample preparation was necessary to enhance bead adsorption. Thus 5 µL of polymer bead suspension in 500 µL were diluted in purified water. Then, 400 µL of this suspension were added on the top of a glass coverslip for 10 min. Unbound beads were removed by washing with water three times. The coverslip was then clamped into a coverslip holder and transferred to the AFM.

AFM and data analysis

AFM measurements were realized in buffer with an Asylum Research MFP-3D atomic force microscope (Asylum Research, Santa Barbara, CA, USA) and a TR400PSA silicon nitride cantilever with a spring constant of 0.08 N/m and a pyramid shaped tip with radius of curvature of 15 nm (Olympus, Tokyo, Japan). Using the integrated fluorescent microscope, DAPI labeled bacteria were identified and an array of force versus indentation curves (force map) was collected. At least 26 individual cells were measured for each species. The particle stiffness was obtained by analyzing a sub-array of 3×3 pixel force versus indentation curves acquired (Fig. 3 and Fig. 4A) in the center of the particle of which at least 4 curves were averaged [27]. The Young's modulus was obtained by a Hertz fit (equations 1 and 2) to the averaged force versus indentation curve. The correlation between the loading force F and indentation δ yields for a conical tip (1) or spherical tip (2) respectively

$$F_{cone} = \frac{E}{1-\nu^2}\frac{2\tan\alpha}{\pi}\delta^2 \quad (2)$$

$$F_{sphere} = \frac{4}{3}\frac{E}{(1-\nu^2)}\sqrt{R}\delta^{\frac{3}{2}} \quad (3)$$

where E is the Young's modulus, v is the Poisson ratio (for which 0.3 was chosen), α is the half opening angle of the conical tip, in our case 18°, R is the radius of the spherical tip, in this case 15 nm.

Depending on the sample, equation 1 or 2 was chosen. When the indentation is much larger than R, which was the case for all bacteria samples, the induced deformation will be dominated by the conical shape of the tip and equation 1 is most appropriate. When the indentation is very small (<R), in case of the polystyrene beads, equation 2 is more accurate since the mean indentation of 5.9 nm at 15 nN was smaller than the tip radius of 15 nm.

To be able to compare the results to literature values, the stiffness (in N/m) of the bacteria and polystyrene beads was also obtained via Hooke's law. For the bacteria, the force versus indentation curves were fitted between 50 and 150 pN loading force, and for the polystyrene beads between 2 and 10 nN. It should be noted that this method is less accurate as it ignores the non-constant contact conditions between the sample and the AFM tip, which is included in the aforementioned Hertz model.

To measure the stiffness of bacteriophages, tapping mode images of a section with multiple single adhered phages were collected (Fig. 4B). At least 4 force versus indentation curves where then collected within the center of the individual phage particle, indicated by the circles. In total, 28 individual phage capsids were measured. The maximum loading force was 500 pN. Previous work on virus mechanics have shown that the non-constant contact conditions between the sample and the AFM tip are less important and that the virus response is linear for small deformations [17]. It can thus be expressed in N/m by fitting the indentation curve between 100 and 250 pN loading force. The relation between this spring constant k and the Young's modulus E follows from a thin shell model that describes the viral protein capsid [17]

$$k = 2.25\frac{Eh^2}{r} \qquad (4)$$

where h is the shell thickness of the phage capsid, r is the radius of the phage, in the present case 10 nm. The radius refers to the center of the shell. Since the structure of PP7 is similar to φ29, 1.6 nm were used for shell thickness h according to [17].

The Olympus TR400PSA 0.08 N/m cantilever used for phages and bacteria was not stiff enough to obtain force versus indentation curves in a reasonable quality for the polystyrene beads. Thus, for these synthetic particles a much stiffer Olympus AC160TS cantilever with 42 N/m was used. With the associated fluorescent microscope, the fluorescently labeled beads were focused and force maps of a section with multiple single adhered beads were collected. In total, 35 individual beads were measured. The maximum loading force was 15 nN. Force maps were evaluated by analyzing a 3×3 pixel area (Fig. 4A) in the center of the beads of which at least 4 force versus indentation curves were used. The Young's modulus was obtained by a Hertz fit analogous to bacteria analysis described above using equation 2.

2.6 Filtration membranes

Standard membranes recommended for robust retention of the respective particle species, i.e. virus- and 0.2 µm sterile filtration membranes, exhibit too high retention degrees to observe changes in the log reduction value (LRV) when the transmembrane pressure is changed. Two membrane layers are commonly used for robust retention in virus filtration. In order to easily detect and differentiate their

retention properties for the different bacteria species, phages and polystyrene particles as a function of TMP, tailor-made, non-commercial, single layer, flat sheet polyethersulfone (PES) precipitation cast membranes of varying nominal pore size from 0.02 – 0.80 µm were used. All membranes were chosen to show either a lower retention, corresponding to a LRV lower than 4 or higher retention corresponding to a LRV higher than 4 for each species at a 200 kPa transmembrane pressure and room temperature.

2.7 Filtration experiments

All filtration experiments were carried out in a dead end, single layered configuration with varying TMP from 10 to 200 kPa at room temperature. The membranes were fitted into polycarbonate syringe filter housings (16517-E, Sartorius Stedim Biotech, Germany) with a membrane diameter of 25 mm and an effective filtration area of 3.14 cm². During filtration, all membranes were challenged with at least 1×10^7 particles per cm² membrane area according to ASTM F838-05 [28] for sterile filter testing.

In order to challenge filtration membranes with bacteria, a respective bacteria culture was diluted with a 0.1 M sodium phosphate buffer, pH 7.1±0.1, so that a titer of approximately 1×10^6 colony forming units per mL (CFU/mL) was reached. The membranes where then challenged with at least 50 mL of the bacteria suspension and a filtrate was collected in sterile tubes. A colony count was carried out using the membrane filtration method described above.

For challenging the filtration membranes with phages, PP7 in TSB was diluted with a 0.02 M potassium phosphate buffer, pH 7.1±0.1, so that a titer of 1×10^6 CFU/mL was reached. Membranes where then challenged with at least 50 mL of the phage suspension and a filtrate was collected in sterile tubes and counted using the plaque assay described above.

The filtration experiments for fluorescent polystyrene beads were carried out using a water suspension containing 0.26% sodium dodecyl sulfate that was obtained by a 2500-fold dilution of the beads stock suspension (2.5% solids). The membranes were challenged with at least 5 mL of the bead suspension.

3 Results and discussion

3.1 Particle size determination by dynamic light scattering and AFM measurements

DLS measurements were realized to verify that the filtered particles were mainly individual particles and free of larger aggregates that could possibly influence the results of the filtration experiments. The measurements of the size of the investigated particles provided reasonable, reproducible, unimodal number particle size distributions for all particle species (Fig. 1). The mean diameters were 19.3 nm for PP7 phage, 191 nm for polystyrene beads, 675 nm for A. laidlawii, 799 nm for B. diminuta and 1118 nm for S. epidermidis (Table 2).

The PP7 phage diameter of 19.3 nm appeared to be lower than values reported in literature, but was consistent with TEM images showing a diameter between 19 and 25 nm (data not shown) and was therefore used to calculate Young's modulus as described in the AFM part of the experimental section. Oshima et al. reported a diameter of 25 nm [29] and Nap et al. used 27.6 nm as an outer diameter for further calculations [30]. In the present study, no further purification of the PP7 phages was carried

out, thus, potentially adventitious particles from phage reproduction could have interfered with the measurements. The measured particle sizes were not compared to the heights measured with the AFM, since the focus was the stiffness of the particles. However, the topographic maps obtained with AFM measurements (Fig. 3 and 4) clearly show heights comparable to the mean diameters measured with DLS (Fig. 1).

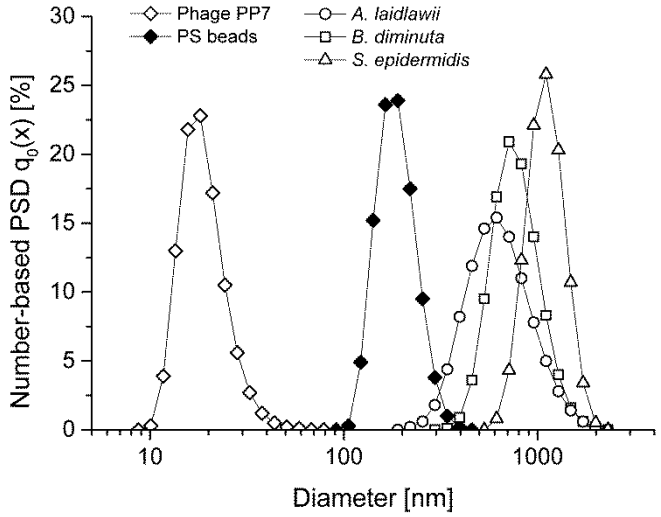

Fig. 1: Averaged number-based particle size distributions obtained from triplicate DLS measurement.

Particle stiffness was measured by AFM in aqueous buffer for all particles employed in this study by generating force maps of the bacteria (Fig. 3) and polystyrene beads (Fig. 4A). Fig. 5A shows representative force versus indentation curves for the three bacteria species. The slope of the curves for the mycoplasma A. laidlawii and Gram-negative B. diminuta were very similar during all experiments. Gram-positive S. epidermidis showed a significantly steeper slope, indicating a higher stiffness. The slopes were used to calculate the spring constants summarized in Table 2. They were 0.0031, 0.0031 and 0.0213 N/m for A. laidlawii, B. diminuta and S. epidermidis, respectively. The values for A. laidlawii and B. diminuta were approximately one order of magnitude lower than the values for other Gram-negative bacteria reported in literature, summarized in Table 3. However, there are no values reported for the species A. laidlawii and B. diminuta. The value of 0.0213 N/m for S. epidermidis was in a good agreement with literature. Francius et al. [31] measured the value of 0.013 N/m for S. aureus, which is a representative of the same species. The small difference could be due to the different buffer that was used in the experiments, thus swelling or shrinking could have affected the measured stiffness.

Deformable particles exhibit a certain resistance against pressure, which is defined by their Young's modulus. The Young's moduli were calculated to compare them with the exerted TMP in the filtration studies. The mean Young's moduli for A. laidlawii, B. diminuta and S. epidermidis were 101±72, 69±34 and 1159±527 kPa, respectively (Fig. 2). While the values for A. laidlawii and B. diminuta were in the same range, S. epidermidis appeared to be an order of magnitude stiffer, which is also indicated by the smaller indentation of approximately 37 nm compared to 105 nm applying the same

maximum loading force of 400 pN. The higher stiffness of Gram-positive S. epidermidis is most likely a result of the thick peptidoglycan layer of 30-100 nm [32], while the cell wall of Gram-negative B. diminuta is only a few nanometers thick [32] and A. laidlawii completely lacks a cell wall. The values of the Gram-negative bacteria and mycoplasma were in a good agreement with the value of 37-210 kPa for S. putrefaciens reported by Gaboriaud et al. [33]. Also the value of S. epidermidis was close to the value of 1746 kPa reported for S. aureus by Francius et al. [31].

Force maps revealed for the latex beads expected narrow distributions of particle size and shape (Fig. 4A). The Young's modulus of the polystyrene beads was approximately 1.6±0.7 GPa, which was close to reported values of 2 to 4 GPa [34].

In the used AFM setup, it was not possible to generate force maps of PP7 phage particles due to the very small phage dimensions. Thus, tapping mode images (Fig. 4B) were generated to determine a center area, indicated by circles, where at least four force versus indentation curves were recorded. Fig. 5B reveals a region where the force suddenly dropped with increasing indentation at 570 pN and 8 nm indentation. This corresponds most likely to a breakage of the brittle capsid as was also observed by Ivanovska et al. for Bacillus subtilis phage φ29 capsid at 1400 pN [17]. In the present study, the behavior was reproducible for all intact PP7 phage capsids. Loading forces for measurements after localization thus never exceeded 500 pN. After successfully capturing the multiple force versus indentation curves of a single capsid, one last measurement was carried out with larger loading forces to force breakage and confirm an intact capsid during prior measurements. The mean phage spring constant was 0.18±0.06 N/m which is in a very good agreement with the values of 0.16 to 0.31 N/m of phage φ29 measured by Ivanovska et al. [17] (Table 2). The capsids are described to be icosahedral and not elongated in literature [21], which was confirmed by TEM images which showed a nearly spherical shape. The Young's modulus was calculated from the spring constant as described in the experimental part. The Young's modulus of phage PP7 was 310 MPa and thus several orders of magnitude higher than for bacteria and only one order of magnitude lower than for polystyrene beads. As described above the phage radius measured with DLS was smaller than reported in literature. However, when the radius is set to 12.5 nm according to Oshima et al. [29] or 13.8 nm according to Nap et al. [30], the Young's modulus is still in the same order of magnitude.

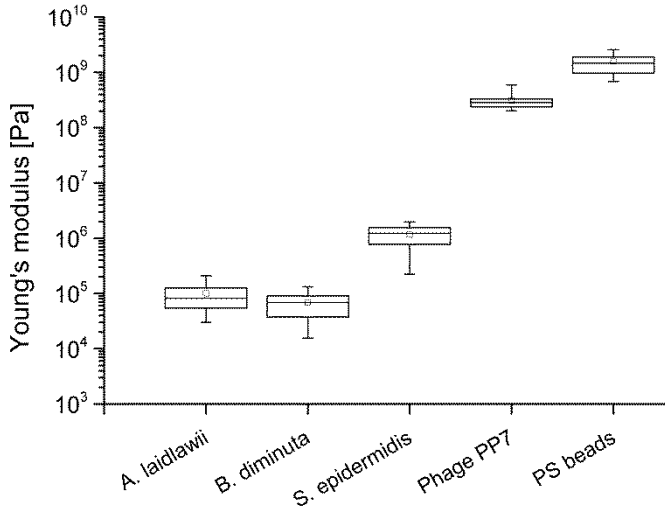

Fig. 2: Box-Whisker plots of the Young's moduli and of bacteria species, bacteriophages and polystyrene beads measured in liquid by AFM (n ≥ 26). Boxes represent the 25th to 75th percentile, the central line the median, the squares represent the mean, and the whiskers represent the 5th and 95th percentile.

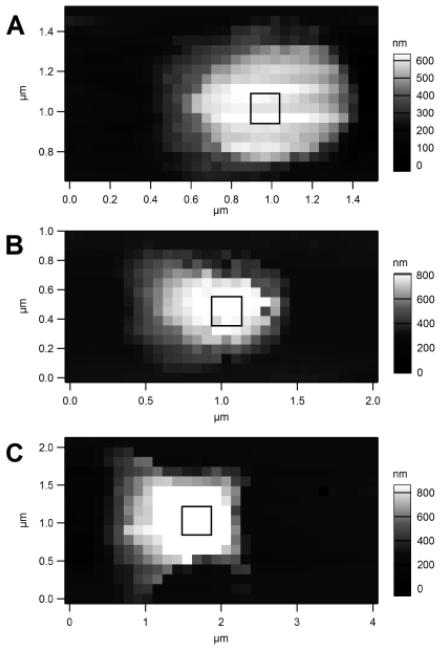

Fig. 3: Representative AFM topographic maps of single bacteria cells: (A) A. laidlawii, (B) B. diminuta, (C) S. epidermidis. Each pixel corresponds to an AFM force versus indentation curve measurement. Notice that image scales are not equal. Squares indicate a 3×3 pixel area in the center of each cell where force versus indentation curves were used to calculate Young's modulus and spring constant. Notice that image scales are not equal.

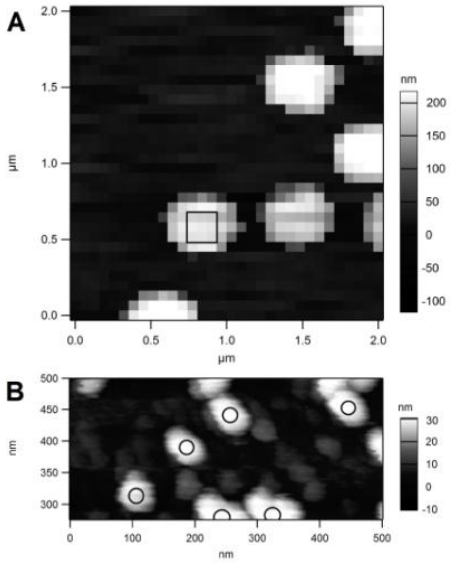

Fig. 4: (A) Representative AFM topographic maps of single polystyrene beads. Each pixel corresponds to a AFM force versus indentation curve measurement. Squares indicate a 3×3 pixel area in the center of each particle where force versus indentation curves were used to calculate Young's modulus and spring constant. (B) Representative AFM tapping mode image of bacteriophages PP7. Circles indicate an area in the center of each phage particle where force versus indentation curves were recorded to calculate the spring constant. Notice that image scales are not equal.

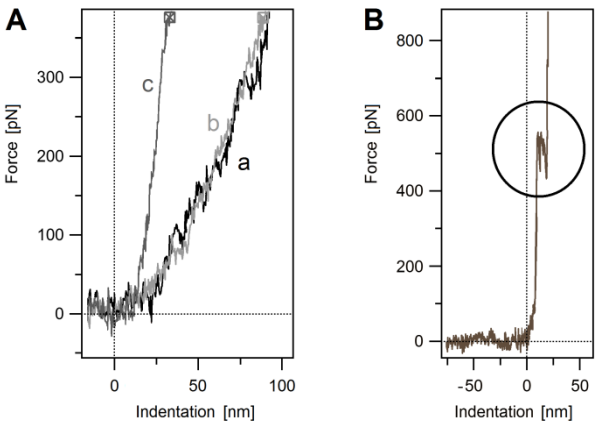

Fig. 5: (A) Representative force versus indentation trace curves of (a) mycoplasma A. laidlawii, (b) Gram-negative B. diminuta and (c) Gram-positive S. epidermidis. Curves for A. laidlawii and B. diminuta show similar slopes, while the slope of S. epidermidis being significantly steeper indicating a higher stiffness. (B) Representative force versus indentation trace curve of PP7 phage capsid. The steep slope indicates a relatively stiff particle. Capsid breakage occurs at approximately 570 pN and 8 nm indentation indicated by the circle, revealing brittleness of the capsid.

Table 2: Sizes and stiffness data of measured particles.

	Acholeplasma laidlawii	Brevundimonas diminuta	Staphylococcus epidermidis	Bacteriophage PP7	Polystyrene beads
Relevant structural properties	No cell wall (lipid bilayer only)	Cell wall (Gram-negative)	Cell wall (Gram-positive)	Rigid protein capsid	Solid material
Mean diameter [nm]	675±19	799±15	1118±84	19.3±1.1	191±2
Cantilever used	Olympus TR400PSA, silicon nitride, 0.08 N/m, pyramidal tip				Olympus AC160TS, silicon, 42 N/m, tetrahedral tip
Mean indentation [nm]	106±42	105±50	37±17	3.2±1.3	5.9±2.2
Maximum loading force [pN]	400	400	400	400	15000
Young's modulus	101±72 kPa (equation 2)	69±34 kPa (equation 2)	1159±527 kPa (equation 2)	310±113 MPa (equation 4)	1.6±0.7 GPa (equation 3)
Spring constant [N/m]	0.0031±0.0014	0.0031±0.0017	0.021±0.013	0.178±0.065	4.87±1.99
Number of individual particles	26	34	26	28	35

Table 3: Published values for the spring constant and Young's modulus of bacteria.

Gram stain	Species	Spring constant [N/m]	Young's modulus [kPa]	Source
Gram-negative	E. coli	0.034-0.044[a]	-	[35]
		0.026[b], 0.069[b]	-	[36], [37]
		-	1.9×10^{3} [c]	[38]
	P. aeruginosa	0.017-0.044[b]	-	[39]
		0.02-0.03[d]	-	[40]
	S. putrefaciens	0.02-0.05[e]	37-210 [e]	[33]
Gram-positive	S. aureus	0.013[c]	1.7×10^{3} [c]	[31]
not applicable	Bacillus subtilis phage φ29	0.16-0.31[f]	1.2×10^{6}-1.6×10^{6} [f]	[17]

[a] Tris buffer, [b] deionized water, [c] PBS buffer, [d] growth medium, [e] potassium nitrate buffer, [f] TMS buffer

3.2 Membrane pore size characterization

In order to evaluate the retentive behavior of the employed biological particle species at a lower and a higher degree of retention, two tailor-made PES membranes were prepared for each species (Table 4). For the rigid polystyrene beads, only one membrane type was prepared (Table 4). The employed membranes were symmetric, i.e. they exhibited no significant pore size gradient over the cross-section of the membrane and a thickness of 120 to 150 µm. This was confirmed by visual evaluation of scanning electron microscopy images of cross-sections generated from freeze-fractured membranes. For illustrative purposes, two representative membrane images are depicted in Fig. 6.

Visual water bubble points ranged from 90 kPa for Epi_low to 470 kPa for Laid_high. Within one bacteria species to test, the more retentive membrane always exhibited a higher bubble point value. Membranes for use with polysytrene beads and phage PP7 exhibited water bubble points above 600 kPa, which could not be determined with the present setup.

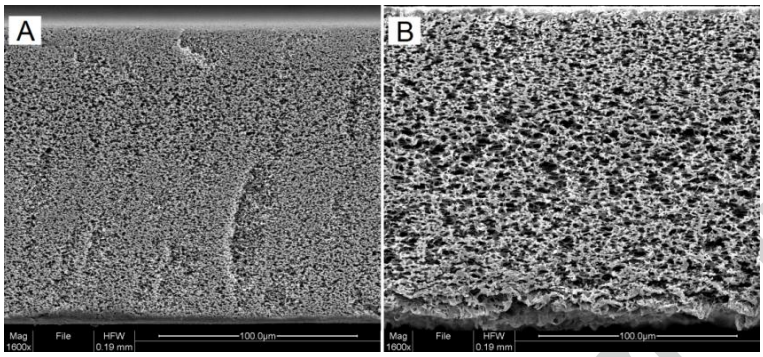

Fig. 6: Cross sectional SEM images of (A) Laid_high membrane and (B) Epi_low membrane.

Table 4: Overview of the single layer PES membranes used.

Membrane name code	Largest pore size diameter [nm]	Mean pore size diameter [nm]	Water bubblepoint [kPa]	Retention degree	Filtered particle species
PP7_high	n.d.	n.d.	>3000[a]	High[a]	P. aeruginosa phage PP7
PP7_low	n.d.	n.d.	>3000[a]	Low[b]	
PSbeads	139	103	>600 [a]	Unspecified	Polystyrene beads
Laid_high	371	298	470	High	A. laidlawii
Laid_low	509	405	330	Low	
Dim_high	613	417	220	High	B. diminuta
Dim_low	983	737	190	Low	
Epi_high	1115	671	150	High	S. epidermidis
Epi_low	1513	941	90	Low	

[a] Theoretical value, [b] High-retention degree corresponds to LRV higher than 4 at room temperature and 200 kPa transmembrane pressure, [c] Low-retention degree corresponds to LRV lower than 4 at room temperature and 200 kPa transmembrane pressure

3.3 Dead-end filtration experiments at different transmembrane pressures

The dead end filtration experiments for each particle species were carried out within a TMP range of 10 to 950 kPa and the membranes listed in Table 4. Differences in retention due to leakage or defective pores can be excluded, since the membranes and membrane housings were integrity tested by the bubble point method.

The first step was to examine the retention behavior of Laid_low as a function of applied TMP, since mycoplasmas were reported to be deformable and in some cases penetrate sterilization grade membranes [11]. Fig. 7 shows the log reduction value of A. laidlawii as a function of TMP for Laid_low. When the TMP was increased from 10 to 200 kPa the LRV significantly decreased from 4.4 to 2.3 log units. Brevundimonas diminuta was chosen as a Gram-negative, but cell wall positive bacteria representative. Here, the LRV significantly dropped from 3.3 to 2.1 for increasing TMP. However, the effect was less distinctive as for the mycoplasma (Dim_low, Fig. 7). For Staphylococcus epidermidis, a Gram-positive bacterium with a thicker peptidoglycan layer, a TMP increase from 10 to 100 kPa yielded no significant LRV decrease, however a slight decrease is visible at 200 kPa (Epi_low, Fig. 7).

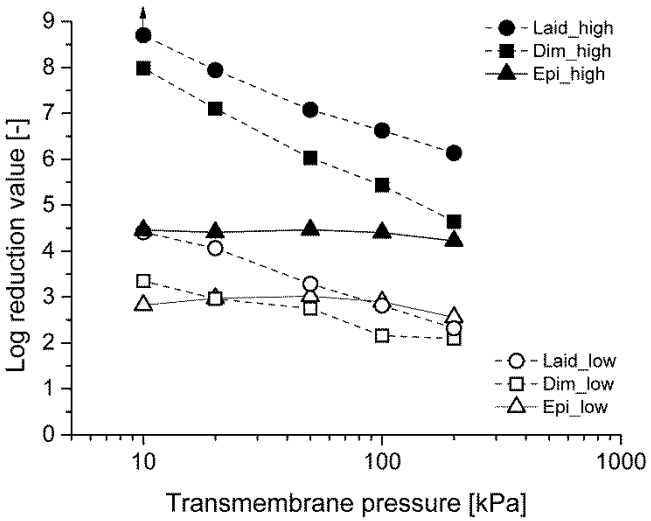

Fig. 7: LRV of bacteria species for low-retention (open symbols) and high-retention (closed symbols) membranes as a function of TMP during filtration of the respective particle species. All symbols represent means of triplicate experiments. The LRV mean standard deviations for A. laidlawii, B. diminuta and S. epidermidis are ±0.3, ±0.3 and ±0.2 log units respectively. Arrows indicate a LRV above the upper detection limit.

The same experiments were also carried out with the respective high-retention membranes (closed symbols in Fig. 7). For A. laidlawii, a significant LRV drop from approximately 8.0 to 6.1 for a TMP increase from 20 to 200 kPa is evident for Laid_high, and comparable to the LRV drop observed for the respective low-retention membrane Laid_low. The LRV at 10 kPa was above the detection limit of approximately 8.7 log units. The high-retention membrane Dim_high used for B. diminuta showed a LRV drop from 8.0 to 4.6 at increasing TMP, which is a difference of 3.4 log units, whereas the LRV drop for the low-retention membrane Dim_low was only 1.2. In general, mycoplasma and the Gram-

negative B. diminuta, showed similar behavior for both low- and high-retention membranes. Gram-positive bacterium S. epidermidis retention was also pressure-independent up to 200 kPa for the high-retention membrane Epi_high.

The AFM measurements revealed that S. epidermidis was an order of magnitude stiffer than A. laidlawii and B. diminuta (Fig. 2, Table 2). The exerted TMP of 200 kPa was therefore possibly not high enough to deform S. epidermidis. Filtration experiments with S. epidermidis where thus carried out with higher TMPs up to 950 kPa, which was in the range of the Young's modulus of 1159 kPa. Fig. 8A shows a significant LRV decrease for S. epidermidis at TMPs above 300 kPa and the LRV decreases from 4.2 to 1.2 log units at a TMP of 950 kPa. The LRV decrease was steeper as for A. laidlawii and B. diminuta. The observed differences in the magnitude of the LRV decrease for the different species could be related to the differences in their envelope structure. Fig. 1 shows that the number-based PSD of S. epidermidis is narrower than that of the other two bacteria species. It could be possible that if the TMP is high enough to deform S. epidermidis cells, more cells of a specific size can pass through the pores and thus the LRV decrease is more pronounced. The Young's moduli of the bacteria species are indicated by arrows in Fig. 8A. It is obvious that the Young's moduli lie amidst the LRV decrease, which is also true for the Laid_high and Dim_high membranes (Fig. 7). Thus deformation already occurs when the TMP is lower than, but in the order of magnitude of the respective Young's modulus. For S. epidermidis significant deformation and LRV decrease starts at a TMP of approximately 25% of its Young's modulus. Since there is no plateau at low TMP for A. laidlawii and B. diminuta it is not possible to determine where their deformation starts.

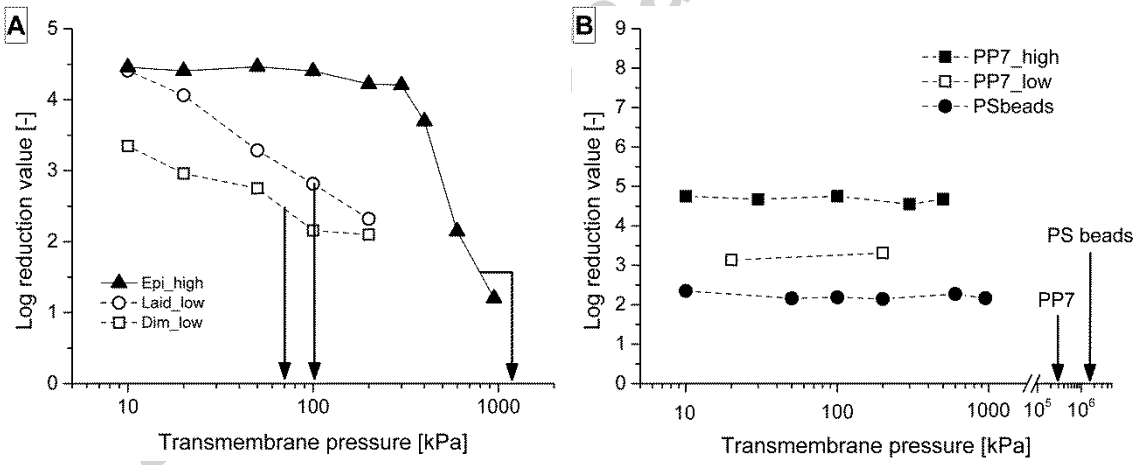

Fig. 8: LRV of (A) bacteria species for low-retention (open symbols) and high-retention (closed symbols) membranes and (B) PP7 bacteriophages and polystyrene beads as a function of TMP during filtration of the respective particle species. All symbols represent means of triplicate experiments. The maximum LRV mean standard deviation is ±0.3 log units. Arrows indicate the Young's modulus of the respective particle species.

Bacteria retention by polymer membranes was found to be TMP-dependent for all bacteria species. The deformability of mycoplasma is supported by Fig. 9 showing significantly elongated A. laidlawii

cells penetrating into small pores of a 0.2 µm track etched polycarbonate membrane after filtration at a TMP of 200 kPa. They have also been reported to be very flexible in literature [41,42].

Lebleu et al. showed that all tested Gram-positive bacteria were retained reliably, while Gram-negative bacteria passed the membrane. The LRV of Gram-negative E. coli using 0.4 µm track-etch membranes decreased from approximately 4.5 to 3 log units when the TMP was increased from 20 to 100 kPa [12]. The LRV actually reached a plateau value already at 50 kPa. E. coli passed the used 0.4 µm track-etch membrane despite being significantly larger than the pores. Gram-positive C. xerosis of the same size and shape did not pass the same membrane. Additionally, this was true for Gram-positive cocci S. aureus and M. luteus, however the TMP never exceeded 100 kPa. Thus, the key drivers for bacteria penetration at higher pressures do not seem to be their shape or relative size, but how the cell envelope is constituted.

Arkhangelsky et al. hypothesized that a possible pore enlargement at high differential pressures could explain the LRV drop [16]. Fig. 10 shows a typical flow performance for Laid_high, Laid_low and Epi_high membranes. The excellent straight-line fit of the flow rate versus pressure relation is a strong indication for constant permeability and thus unchanged pore size over the exerted TMP range which is also true for pressures up to 950 kPa for the Epi_high membrane (Fig. 10B).

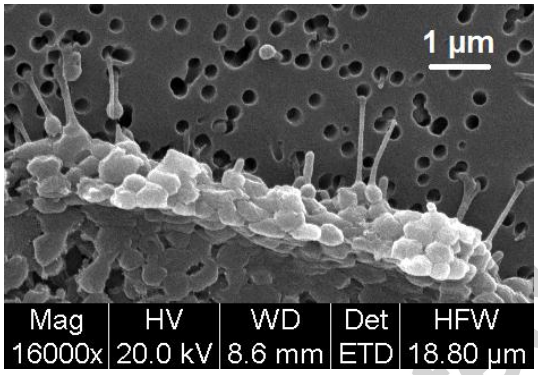

Fig. 9: Scanning electron microscope image of Acholeplasma laidlawii cells penetrating pores of a 0.2 µm polycarbonate track etched membrane. Cells were fixed with glutaraldehyde and dewatered with increasing ethanol concentrations after filtration at 200 kPa TMP.

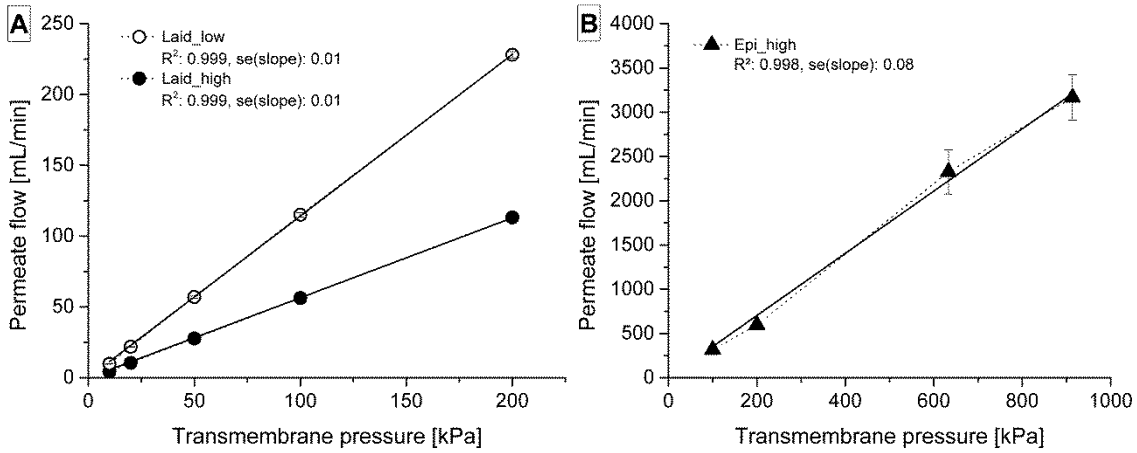

Fig. 10: Permeate flow rate as a function of applied TMP for (A) Laid_high and Laid_low and (B) Epi_high. Error bars represent standard deviations of the individual data. A straight-line with origin intersect was fitted to the data.

Compared to bacteria, polystyrene beads are stiff and hardly deformable particles. AFM measurements presented above confirmed these findings. Accordingly, Fig. 8B shows no TMP dependency of the LRV for these particles up to a TMP of 950 kPa. The same phenomenon was observed for bacteriophage PP7 particles for both membrane types. Phages were reported to be stiff [17] but no deformability values were given. As was shown above, phages were several orders of magnitude stiffer than bacteria, which makes their stiffness comparable to that of polystyrene. The Young's moduli of both polystyrene beads and phages were several orders of magnitude higher and thus far away from the maximum exerted TMPs of 950 and 500 kPa (Fig. 8B). The independence of LRV of the stiff particles and phages on TMP supports the hypothesis that the LRV drop observed for bacteria was caused by their deformation. If there were any interactions that would correlate with membrane-particle contact times, an LRV drop should also be observed with bacteriophage PP7. If adsorption played a role in a LRV drop, this would occur for phages due to capsid protein-membrane-interactions.

4 Conclusions

This study, for the first time, provides experimental stiffness data for a wide range of different biological and non-biological model particles, ranging 20 – 1500 nm in size. Using the same AFM methodology enables a direct comparison of stiffness and thus deformability of those different particle species. The data shows, that mycoplasma A. laidlawii and Gram-negative B. diminuta are relatively soft (Young's modulus of 101 and 69 kPa), while Gram-positive S. epidermidis is one order of magnitude stiffer (Young's modulus of 1159 kPa), most likely due to its thick peptidoglycan layer. PP7 bacteriophages and polystyrene beads are two to three orders of magnitude stiffer than bacteria (Young's modulus of 310 and 1577 MPa). This paper shows that the impact of TMP on particle retention in dead end microfiltration is strongly correlated to particle stiffness; the stiffer a particle, the lesser is the impact of TMP on particle retention. A. laidlawii and common Gram-negative B. diminuta

bacteria exhibit low particle stiffness and therefore, increasing TMP leads to significantly decreased levels of retention. Gram-positive bacteria S. epidermidis are one order of magnitude stiffer than A. laidlawii and B. diminuta and their retention is only dependent on TMP when pressures greater than 300 kPa are used. Phages and latex beads, being even stiffer than S. epidermidis, did not show retention dependence on TMP within the tested range. The used tailor-made membranes in single-layer configuration enabled detailed insight into LRV changes when the TMP was changed. The generated physical data and the related correlation to particle retention supports the mostly empirical expectation that mycoplasma and Gram-negative bacteria retention can be elevated when sterile filtration processes are carried out at lower TMP values.

Acknowledgements

The authors thank Dr. Wiebke Möbius of the Max-Planck Institute of Experimental medicine, Goettingen, Germany for preparing the transmission electron microscopy images of PP7 phage.

References

[1] A. Berting, M.R. Farcet, T.R. Kreil, Virus susceptibility of Chinese hamster ovary (CHO) cells and detection of viral contaminations by adventitious agent testing., Biotechnol. Bioeng. 106 (2010) 598–607. doi:10.1002/bit.22723.

[2] J. Fogh, N. Holmgren, P. Ludovici, A review of cell culture contaminations, In Vitro. 7 (1971) 26–41. doi:10.1007/BF02619002.

[3] R.L. Garnick, Raw materials as a source of contamination in large-scale cell culture., Dev. Biol. Stand. 93 (1998) 21–29.

[4] R.L. Garnick, Experience with viral contamination in cell culture., Dev. Biol. Stand. 88 (1996) 49–56.

[5] E. Langer, Biotech facilities average a batch failure every 40.6 weeks, Bioprocess Int. 6 (2008).

[6] A. Kumar, S. Egli, J. Martin, C. Golightly, R. Kuriyel, L. Sciences, Contamination Costs, Eur. Biopharm. Rev. (2009) 68–74.

[7] P. Blosse, Meeting The New Challenges of Sterilising by Filtration, Pharm. Manuf. Int. (2000) 117–119.

[8] C.F. Nnadozie, J. Lin, R. Govinden, Selective isolation of bacteria for metagenomic analysis: Impact of membrane characteristics on bacterial filterability, AIChE J. (2015) 853–866. doi:10.1002/btpr.2109.

[9] T. Hirasaki, T. Noda, H. Nakano, Y. Ishizaki, Mechanism of Removing Japanese Encephalitis virus (JEV) and Gold Particles Using Cuprammonium Regenerated Cellulose Hollow Fiber (i-BMM or BMM) from Aqueous Solution, Polym. J. 26 (1994) 1244–1256. doi:10.1295/polymj.26.1244.

[10] S.R. Wickramasinghe, E.D. Stump, D.L. Grzenia, S.M. Husson, J. Pellegrino, Understanding virus filtration membrane performance, J. Memb. Sci. 365 (2010) 160–169. doi:10.1016/j.memsci.2010.09.002.

[11] M. Folmsbee, M. Moussourakis, Retention of Highly Penetrative A. laidlawii Mycoplasma Cells, Bioprocess Int. 10 (2012) 60–62.

[12] N. Lebleu, C. Roques, P. Aimar, C. Causserand, Role of the cell-wall structure in the retention of bacteria by microfiltration membranes, J. Memb. Sci. 326 (2009) 178–185. doi:10.1016/j.memsci.2008.09.049.

[13] X. Sun, W.D. Weinlandt, H. Patel, M. Wu, C.J. Hernandez, A microfluidic platform for profiling biomechanical properties of bacteria., Lab Chip. 14 (2014) 2491–2498. doi:10.1039/c3lc51428e.

[14] S.S. Madaeni, A.G. Fane, G.S. Grohmann, Virus removal from water and wastewater using membranes, J. Memb. Sci. 102 (1995) 65–75. doi:10.1016/0376-7388(94)00252-T.

[15] M. Azari, J.A. Boose, K.E. Burhop, T. Camacho, J. Catarello, A. Darling, et al., Evaluation and validation of virus removal by ultrafiltration during the production of diaspirin crosslinked haemoglobin (DCLHb)., Biologicals. 28 (2000) 81–94. doi:10.1006/biol.2000.0246.

[16] E. Arkhangelsky, V. Gitis, Effect of transmembrane pressure on rejection of viruses by ultrafiltration membranes, Sep. Purif. Technol. 62 (2008) 619–628. doi:10.1016/j.seppur.2008.03.013.

[17] I.L. Ivanovska, P.J. de Pablo, B. Ibarra, G. Sgalari, F.C. MacKintosh, J.L. Carrascosa, et al., Bacteriophage capsids: tough nanoshells with complex elastic properties., Proc. Natl. Acad. Sci. U. S. A. 101 (2004) 7600–5. doi:10.1073/pnas.0308198101.

[18] S. Nawaz, P. Sánchez, K. Bodensiek, S. Li, M. Simons, I.A.T. Schaap, Cell visco-elasticity measured with AFM and optical trapping at sub-micrometer deformations., PLoS One. 7 (2012). doi:10.1371/journal.pone.0045297.

[19] V. Vadillo-Rodríguez, J.R. Dutcher, Viscoelasticity of the bacterial cell envelope, Soft Matter. 7 (2011) 4101–4110. doi:10.1039/c0sm01054e.

[20] I.A.T. Schaap, C. Carrasco, P.J. de Pablo, F.C. MacKintosh, C.F. Schmidt, Elastic response, buckling, and instability of microtubules under radial indentation., Biophys. J. 91 (2006) 1521–1531. doi:10.1529/biophysj.105.077826.

[21] K. Tars, K. Fridborg, M. Bundule, L. Liljas, The three-dimensional structure of bacteriophage PP7 from Pseudomonas aeruginosa at 3.7-A resolution., Virology. 272 (2000) 331–337. doi:10.1006/viro.2000.0373.

[22] P.Y. Liu, L.K. Chin, W. Ser, T.C. Ayi, P.H. Yap, T. Bourouina, et al., Real-Time measurement of single bacterium's refractive index using optofluidic immersion

refractometry, Procedia Eng. 87 (2014) 356–359. doi:10.1016/j.proeng.2014.11.743.

[23] L. Daneo-Moore, D. Dicker, M.L. Higgins, Structure of the nucleoid in cells of Streptococcus faecalis, J. Bacteriol. 141 (1980) 928–937.

[24] J.A.C. Valkenburg, C.L. Woldringh, Phase separation between nucleoid and cytoplasm in Escherichia coli as defined by immersive refractometry, J. Bacteriol. 160 (1984) 1151–1157.

[25] A.E. Balaev, K.N. Dvoretski, V.A. Doubrovski, Determination of refractive index of rod-shaped bacteria from spectral extinction measurements, in: Saratov Fall Meet. 2002 Opt. Technol. Biophys. Med. IV, 2003: pp. 375–380. http://dx.doi.org/10.1117/12.518853.

[26] K.F.A. Ross, The Size of Living Bacteria, Q. J. Microsc. Sci. 98 (1957) 435–454. http://jcs.biologists.org/content/s3-98/44/435.abstract.

[27] S. Li, F. Eghiaian, C. Sieben, A. Herrmann, I.A.T. Schaap, Bending and puncturing the influenza lipid envelope., Biophys. J. 100 (2011) 637–645. doi:10.1016/j.bpj.2010.12.3701.

[28] Standard test method for determining bacterial retention of membrane filters utilized for liquid filtration. ASTM Standard F838-05., Philadelphia, PA, 2013.

[29] K.H. Oshima, T.T. Evans-Strickfaden, A.K. Highsmith, E.W. Ades, The removal of phages TI and PP7, and poliovirus from fluids with hollow-fiber ultrafilters with molecular weight, Can. J. Microbiol. 41 (1995) 316–322. doi:10.1139/m95-044.

[30] R.J. Nap, A.L. Božič, I. Szleifer, R. Podgornik, The role of solution conditions in the bacteriophage pp7 capsid charge regulation, Biophys. J. 107 (2014) 1970–1979. doi:10.1016/j.bpj.2014.08.032.

[31] G. Francius, O. Domenech, M.P. Mingeot-Leclercq, Y.F. Dufrêne, Direct observation of Staphylococcus aureus cell wall digestion by lysostaphin, J. Bacteriol. 190 (2008) 7904–7909. doi:10.1128/JB.01116-08.

[32] T.J. Silhavy, D. Kahne, S. Walker, The bacterial cell envelope, Cold Spring Harb. Perspect. Biol. 2 (2010) 1–16. doi:10.1101/cshperspect.a000414.

[33] F. Gaboriaud, S. Bailet, E. Dague, F. Jorand, Surface structure and nanomechanical properties of Shewanella putrefaciens bacteria at two pH values (4 and 10) determined by atomic force microscopy., J. Bacteriol. 187 (2005) 3864–8. doi:10.1128/JB.187.11.3864-3868.2005.

[34] I. Oral, H. Guzel, G. Ahmetli, Measuring the Young's modulus of polystyrene-based composites by tensile test and pulse-echo method, Polym. Bull. 67 (2011) 1893–1906. doi:10.1007/s00289-011-0530-z.

[35] S.B. Velegol, B.E. Logan, Contributions of bacterial surface polymers, electrostatics, and cell elasticity to the shape of AFM force curves, Langmuir. 18 (2002) 5256–5262.

doi:10.1021/la011818g.

[36] V. Vadillo-Rodriguez, S.R. Schooling, J.R. Dutcher, In situ characterization of differences in the viscoelastic response of individual gram-negative and gram-positive bacterial cells, J. Bacteriol. 191 (2009) 5518–5525. doi:10.1128/JB.00528-09.

[37] M.A. Beckmann, S. Venkataraman, M.J. Doktycz, J.P. Nataro, C.J. Sullivan, J.L. Morrell-Falvey, et al., Measuring cell surface elasticity on enteroaggregative Escherichia coli wild type and dispersin mutant by AFM, Ultramicroscopy. 106 (2006) 695–702. doi:10.1016/j.ultramic.2006.02.006.

[38] A. Cerf, J.C. Cau, C. Vieu, E. Dague, Nanomechanical properties of dead or alive single-patterned bacteria, Langmuir. 25 (2009) 5731–5736. doi:10.1021/la9004642.

[39] V. Vadillo-Rodriguez, T.J. Beveridge, J.R. Dutcher, Surface viscoelasticity of individual gram-negative bacterial cells measured using atomic force microscopy., J. Bacteriol. 190 (2008) 4225–4232. doi:10.1128/JB.00132-08.

[40] X. Yao, J. Walter, S. Burke, M.H. Jericho, D. Pink, R. Hunter, et al., Atomic force microscopy, computer simulations and theoretical considerations of the surface properties and turgor pressures of bacteria, Colloids Surf. B Biointerfaces. 23 (2002) 213–230.

[41] U. Fürnkranz, K. Siebert-Gulle, R. Rosengarten, M.P. Szostak, Factors influencing the cell adhesion and invasion capacity of Mycoplasma gallisepticum., Acta Vet. Scand. 55 (2013) 63. doi:10.1186/1751-0147-55-63.

[42] S. Sundaram, M. Auriemma, G. Howard, Application of membrane filtration for removal of diminutive bioburden organisms in pharmaceutical products and processes, PDA J. Pharm. Sci. Technol. 53 (1999) 186–201. http://journal.pda.org/content/53/4/186.short (accessed February 2, 2015).

Highlights

- The retention of a broad range of different particles, ranging from 0.02 to 1.5 µm in size (mycoplasma, Gram-negative and –positive bacteria, bacteriophages, polystyrene beads), by PES MF membranes was studied for different transmembrane pressures.
- Particle stiffness was determined for the entire range of particles by one unified AFM method enabling direct comparison of stiffness values.
- An observed decrease of particle retention by microfiltration membranes at increasing transmembrane pressure can be correlated to particle softness.